Thin Solid Films 715 (2020) 138419

Contents lists available at ScienceDirect

Thin Solid Films

journal homepage: www.elsevier.com/locate/tsf

Compact protein (bovine serum albumin/human serum albumin) layer under Langmuir-Blodgett deposition on hydrophilic Si (001) surface

Raktim J. Sarmah, Bijay K. Sah, Sarathi Kundu *

Soft Nano Laboratory, Physical Sciences Division, Institute of Advanced Study in Science and Technology, Vigyan Path, Paschim Boragaon, Garchuk, Guwahati, Assam 781035, India

ARTICLE INFO

Keywords:
Bovine serum albumin
Human serum albumin
Monolayer
Proteins
Thin films
Langmuir-Blodgett method
Out-of-plane structures
Protein layer growth

ABSTRACT

Langmuir monolayers of globular proteins (bovine serum albumin, i.e., BSA and human serum albumin, i.e., HSA) are formed on the water surface at pH ≈ 7.0, and compact protein layers are deposited on hydrophilic Si (001) surface using the Langmuir-Blodgett deposition method. Stability of these protein monolayers are studied from the normalized molecular area-time (A/A_0-t) curves, which confirms that deposition over a long period of time is possible from both the protein monolayers. Compact bimolecular layered structure of the protein films are deposited on Si surface at higher surface pressure (17 mN/m) of the BSA and HSA monolayers, which is confirmed from the electron density profiles (EDPs) obtained from the analysis of the X-ray reflectivity data. Mostly the thickness of the molecular layers increases as the molecular tilting takes place and new molecules are deposited inside the vacant positions of the layer and as a result the electrons per unit area increases. EDPs obtained from the deposited BSA and HSA films also confirm that the increment in molecular tilting and electrons per unit area is protein specific. EDPs and surface morphology obtained from the atomic force microscopy images of the deposited films confirm that interrupted layer-by-layer or Frank-van der Merwe growth mode is followed in such protein multilayer deposition.

1. Introduction

Proteins are biomolecules that play an important role in living organisms. Different protein adsorption processes are studied on solid surfaces which serve as a primary step in the formation of biofilms. Investigations on the formation of such protein films are important as it has various practical applications in the fields of medicine, engineering and food processing [1]. Edible films grown from renewable and natural polymers such as proteins can be used to reduce the loss of moisture in food products, packaging materials, etc. [2]. Studies on adsorbed protein films on solid surfaces are also important and relevant in the applications of biosensors and chromatographic separations of various antibodies, drugs and peptides [3-9]. Variation of surface charge and hydrophobic/hydrophilic parts of proteins effectively controls such protein adsorption on different surfaces. The surface charge of proteins can be easily tuned by varying the pH of the solution, however it becomes neutral at a particular pH called isoelectric point [10]. The charged groups are not distributed uniformly on the protein surface, instead they are grouped in patches to form a complex pattern. Structurally, proteins are large amphipathic molecules having polar, non-polar and ionic regions. Due to the presence of these regions, they easily get attached to different surfaces [11]. Protein adsorption can be well understood by studying the various structures, conformations and functions of proteins [10,12,13]. Among all the proteins, serum albumin is the only protein found abundantly in the blood plasma [14].

Globular proteins even after water soluble can form Langmuir monolayer at the air-water interface [15] and their out-of-plane structures at different surface pressures and subphase pH conditions are studied after depositing the films on solid surfaces by Langmuir-Blodgett (LB) method [16-21]. Among different globular proteins, bovine serum albumin (BSA) and human serum albumin (HSA) are the widely studied proteins. The molecular weight of BSA is ≈ 66.5 kD and it contains 582 amino acid residues [22]. The isoelectric point (pI) of BSA is ≈ 4.8 and the molecule can be divided into three main domains, where each domain has different charge densities which is pH dependent. As a result, the variation in pH can affect the shape and size of the molecule [23]. pH dependent conformational changes of proteins were also evidenced by previous studies. It has been observed that conformational changes generally occurs below pH ≈ 4.0 [24,25] and for BSA its structure remains unaltered within pH ≈ 4.0 to 9.0 having a

* Corresponding author.
E-mail address: sarathi.kundu@gmail.com (S. Kundu).

https://doi.org/10.1016/j.tsf.2020.138419
Received 26 March 2020; Received in revised form 14 October 2020; Accepted 21 October 2020
Available online 9 November 2020

concentration range of 10-50 mg/ml [24]. HSA is the abundant protein found in blood plasma and consists of 585 amino acids having a molecular weight of ≈ 66.5 kD and isoelectric point of ≈ 4.8. Approximately 76% homology sequence is displayed by both HSA and BSA molecules along with the conservation of the repeating pattern of the disulphides. Higher affinity of HSA to different ions and small molecules like Cu^{2+} and Zn^{2+} ions, fatty acids, amino acids and metabolites such as bilirubin in solution has been revealed [26].

The deposition of such globular proteins on some solid surfaces and understanding their assembly after deposition is essential from both basic and applied point of view. It is still not yet clear what kind of growth occurs in such a protein multilayer deposition process on the hydrophilic silicon surface. Different growth models exist for the heteroepitaxial film growth on solid substrates [27,28]. Mainly the surface and the interface energies are the two parameters that govern the growth modes. If the surface energy of the substrate (γ_1) is greater than the sum of the epilayer surface energy (γ_2) and the interface energy (γ_{12}), i.e., $\gamma_1 > \gamma_2 + \gamma_{12}$, then this condition is referred to as wetting condition. Under this condition, layer-by-layer growth or Frank-van der Merwe (FM) mode occurs. If this condition does not hold, then there is an increase in surface energy in the layer, then island growth or Volmer-Weber growth occurs. On the contrary, when the wetting condition is satisfied but large strain energy in the upper layer is developed in the layer-by-layer growth, then for lowering its energy, isolated islands are formed above the wetting layer. In this case, Stranski-Krastanow growth mode, i.e., a wetting layer along with islands occurs. Corresponding to the different growth nature complex patterns are developed, which are often observed in different physical systems and thin film deposition methods. Like inorganic materials, different growth modes are also proposed to happen for organic molecules [29–31]. Analysis of such structures and patterns are made using different scattering and microscopic techniques. The growth mechanism of the LB films of fatty acid salts are explored using X-ray scattering and atomic force microscopic studies [32,33]. Moreover, growth under monolayer collapse and the corresponding growth mechanisms are also explored, where Stranski-Krastanow growth nature is identified under the collapse of fatty acid salt monolayer [34]. Like fatty acid salts, the structure and nature of layer-by-layer growth of cholesterol monolayer on the solid surface has also been studied [35]. Although the growth nature and possibility of layer-by-layer deposition are studied for different organic monolayers, but there is no such study for the globular proteins monolayer.

In this article, we have deposited BSA and HSA films by standard Langmuir-Blodgett (LB) deposition method on hydrophilic silicon (001) substrates and both the out-of-plane structure and in-plane morphology of the films are explored from X-ray reflectivity (XRR) and atomic force microscopy (AFM) respectively. The protein Langmuir monolayers formed at the air-water interface were transferred onto the hydrophilic Si substrates by successive up and down strokes (both odd and even numbers) of the substrate through the monolayer covered water surface. All the films were deposited at a subphase pH ≈ 7.0, which is well above the isoelectric point of both the protein molecules and at a control pressure of 17 mN/m at room temperature (≈ 24°C). A highly compact protein bimolecular layer structure is formed on the solid surface, which is obtained from both the out-of-plane structure and in-plane morphology of the deposited protein films. A probable reason for forming such a specific bimolecular layer and growth nature under LB deposition is also explored.

2. Experimental

BSA (catalog No. A2153) and HSA (catalog No. A3782) were purchased from Sigma-Aldrich and were used without further purification. The average molecular weight of both BSA and HSA molecule is ≈ 66.5 kDa. Both BSA and HSA solutions of concentration 1 mg/ml were prepared by dissolving the required amount of protein molecules in phosphate buffer solutions before each experiment and was carefully spread with the help of a syringe on the surface of aqueous subphase in a double-barrier Langmuir trough made of Teflon (Apex Instruments). The trough dimension was ≈ 56.5 cm (length) × 19.5 cm (width) × 0.5 cm (height), having a well of dimension ≈ 8.0 cm (length) × 6.0 cm (width) × 5.5 cm (height). A paper Wilhelmy plate was used to record any changes in the surface pressure. Monolayers were compressed and expanded at a constant speed of 5 mm/min during the isotherm measurements and film deposition. Before each deposition, a time lapse of about 15 min was set for the monolayers to gain stability. To make the substrates hydrophilic, Si (001) substrates were cleaned properly keeping it in a mixed solution of ammonium hydroxide (NH_4OH, Merck, 30%), hydrogen peroxide (H_2O_2, Merck, 30%) and ultra pure water (H_2O: NH_4OH: H_2O_2 = 2:1:1, by volume) for 5–10 min at 100°C. All the substrates were kept inside the ultra pure water until LB deposition after cleaning. All surface pressure (π) – specific molecular area (*A*) isotherm measurements and film depositions were done at room temperature of ≈ 24°C. For different experimental conditions and depositions, the pH of the water subphase was maintained at ≈ 7.0 using phosphate buffer solution. The films were deposited on silicon substrates by LB method at a constant surface pressure of ≈ 17 mN/m. This pressure is chosen for having a relatively compact protein monolayer for better deposition before reaching the limiting positions of the barriers. Depositions of the protein layer were carried out by successive up stroke (US) and down stroke (DS) of the substrate through the protein monolayer covered water surface and it was continued from single upstroke (1US) up to twelve down/up strokes (6DS+6US). Monolayer deposited by single up stroke is designated as 1US, whereas from bilayer to up to twelve layers deposited by different numbers of down-up and up-down cycles of the substrates are designated as 1DS+1US, 2US+1DS, 2DS+2US, 3US+2DS, 3DS+3US, 4US+3DS, 4DS+4US, 5US+4DS, 5DS+5US, 6US+5DS and 6DS+6US respectively. A relaxation time of about 5 min was set above the subphase after each deposition. In the down stroke the substrate goes from air to water and in the up stroke the substrate goes from water to air through the protein monolayer. The speed for both the strokes was 2 mm/min.

Surface topography of all the deposited films of BSA and HSA were studied through atomic force microscopy (NTEGRA Prima, NT-MDT Technology) in semi-contact mode using silicon cantilever having a spring constant of ≈ 11.8 N/m [36]. The images were obtained under ambient condition in air at room temperature. The scans were carried out in a constant force mode over several portions of the film with scan area of 1μm × 1μm for all the deposited protein films. For AFM image processing and analysis, WSxM software [37] was used.

X-ray reflectivity (XRR) measurements of BSA and HSA thin films were carried out using an X-ray diffractometer setup. Diffractometer (D8 Advanced, Bruker AXS) has a copper (Cu) source sealed in a tube followed by a Göbel mirror for the selection and enhancement of the Cu K_α radiation (≈1.54 Å). For detecting the scattered beam NaI scintillation (point) detector was used. Data were taken in specular condition, i.e., the incident angle (θ) was kept equal to the reflected angle (θ) such that both lie in the same scattering plane. Under such condition, a non-vanishing wave-vector component, q_z, is given by $(4\pi/\lambda)\sin\theta$. Analysis of XRR data was pursued using Parratt's formalism [38] where the film is supposed to be a stack of multiple homogeneous layers with sharp interfaces. However, to analyze the XRR data, surface and interfacial roughness are included [39,40]. XRR data effectively provides electron density variation, i.e., the electron-density profile (EDP) [39,41] which is in-plane (*x*–*y*) average electron density (ρ) as a function of depth (*z*) with high resolution [39–43]. From the EDPs, out-of-plane structures of the deposited films are obtained. In general, the electron density variation in a specimen is determined by assuming a model and comparing the simulated reflectivity profile with the experimental data. In this formalism, EDP is extracted from the fitting of the experimental XRR data. For the data fitting, each film was divided into a number of layers including roughness at each interface. The density of Si substrate and the

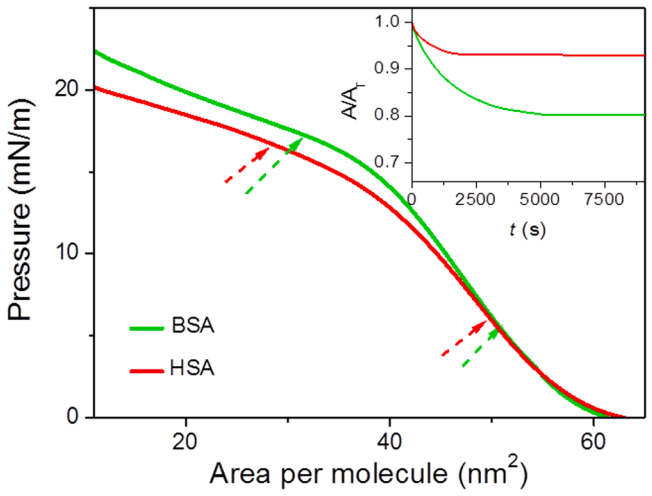

Fig. 1. Surface pressure-specific molecular area (π–A) isotherms of BSA and HSA monolayers on an aqueous subphase of pH ≈ 7.0. Inset: stability curves of BSA and HSA monolayers at a constant surface pressure (π ≈ 17 mN/m). Arrows indicate the points at which films are deposited by the LB method.

density of thin (≈ 24 Å) silicon oxide layer formed on the Si surface were kept constant during data fitting. The density of BSA and HSA were varied but it was less than the maximum density obtained in dry condition. For the 1US and 1DS+1US films three-layer model was used, whereas for all remaining films six-layer model was used for better fitting as air-film, film-substrate and film-film interfaces may have different electron density and roughness values. An instrumental resolution in the form of a Gaussian function and a constant background were also included at the time of data analysis.

3. Results and discussion

The surface pressure-specific molecular area (π–*A*) isotherms of BSA and HSA proteins are shown in Fig. 1. The isotherms were taken at subphase pH ≈ 7.0, which is well above the isoelectric point of both the protein molecules (pI ≈ 4.8). The surface pressure starts to rise at about 62 nm^2/molecule and then starts to increase relatively sharply. If the structure of BSA is considered as an oblate ellipsoid of radii $a \times a \times b \approx$ 39 Å × 39 Å × 9 Å [44], then the calculated A_0 will be $\pi a^2 \approx 47.8$ nm^2. It thus implies that the surface pressure starts to increase from higher *A* before the compact A_0 value, probably due to the electrostatic repulsive interaction. The increase in surface pressure is observed as the area/-molecule goes on decreasing and the monolayer starts to become compact as the molecules come closer to each other depending upon their hydrophobicity and surface charge. When the area is decreased below ≈ 40 nm^2/molecule, a change in slope in the isotherms occurs for both the protein monolayers. At this point a rapid decrease in the slope is observed forming a plateau-like feature. For BSA, the plateau-like feature is observed at a surface pressure of 15-18 mN/m at pH ≈ 7.0, whereas for HSA it is shifted towards a little lower value. Such a plateau-like feature indicates the formation of molecular tilting or molecular reorganization around that point, since molecular desorption does not take place and the stability of the protein monolayer has been checked by compression/decompression isotherm cycle (data not shown). The plateau-like feature is again followed by the rise in surface pressure up to the barrier limits. Comparison shows that the nature of the isotherms for both the protein monolayers is nearly similar except for the maximum attainable surface pressure value. In the inset of Fig. 1, the stability of both the BSA and HSA protein monolayers formed at the air-water interface are shown by the normalized specific molecular area-time (A/A_0-t) curves at a constant surface pressure of 17 mN/m. Stability curves for both the protein monolayers are shown for a period of ≈ 150 min at room temperature. From the stability curves it is observed that for the same constant pressure the area loss by the HSA monolayer is less (≈ 5%) than that of BSA monolayer (≈ 18%). However, it can be concluded that the stability of both BSA and HSA monolayers is sufficient enough to form monolayer to multilayer deposition on solid substrates by LB method.

To obtain the surface morphology and out-of-plane structures of compact BSA and HSA films, both the protein molecules were deposited on hydrophilic Si (001) substrates at a target pressure of 17 mN/m. We have chosen this higher value of the target pressure as the deposition is generally possible from the compact monolayer which provides better transfer efficiency. Protein monolayer was also deposited at lower surface pressure, i.e., before the plateau at 5 mN/m to compare the out-of-plane structure with the films deposited at a higher surface pressure of 17 mN/m. The monolayer formed on the water surface was transferred to the Si (001) substrates by single up stroke (1US). To form the layered structure by conventional LB method from the Langmuir monolayer, both odd and even numbers of BSA and HSA layers were deposited by successive up and down strokes of the substrate through the monolayer covered water subphase, i.e., 1US to 6DS+6US films are prepared. Successful transfer of the monolayer to the solid substrates is known from the transfer ratio (TR) values, however, the details of structures and morphology of the deposited films are obtained from the different scattering, microscopic and spectroscopic techniques. It can be seen that the TR values of the deposited films up to sixth stroke, i.e., up to 3US+3DS films for both the monolayers are within the range of 0.12 – 1.05, where the maximum TR value of ≈ 1.05 is obtained for the 1US film, whereas it is always very less (0.12-0.35) for the down strokes and is higher for the up strokes (0.68-1.05), which implies that the deposition is negligible during down strokes. TR values suggest that the interaction between the hydrophilic substrate and the protein molecules are strong, but the protein-protein interaction above fifth stroke may be weaker to support multilayer formation. With increase in the number of down/up stroke of deposition beyond the fifth stroke, TR value always shows a lower value (0.11-0.32) in each stroke, implying that protein-protein interaction becomes weaker. All the TR values for the BSA and

Table 1
Transfer ratio (TR) values for different up and down strokes during the deposition of bovine serum albumin (BSA) multilayers.

Name of the films	TR values for the BSA layer deposition [US → up stroke and DS → down stroke]											
1US	1.01 (US)											
1DS + 1US	0.30 (DS)	0.91 (US)										
2US + 1DS	1.04 (US)	0.24 (DS)	0.87 (US)									
2DS + 2US	0.31 (DS)	0.98 (US)	0.22 (DS)	0.88 (US)								
3US + 2DS	0.98 (US)	0.26 (DS)	0.87 (US)	0.19 (DS)	0.78 (US)							
3DS + 3US	0.29 (DS)	1.02 (US)	0.21 (DS)	0.85 (US)	0.22 (DS)	0.33 (US)						
4US + 3DS	0.99 (US)	0.27 (DS)	0.88 (US)	0.17 (DS)	0.79 (US)	0.20 (DS)	0.30 (US)					
4DS + 4US	0.35 (DS)	1.01 (US)	0.20 (DS)	0.88 (US)	0.19 (DS)	0.36 (US)	0.17 (DS)	0.29 (US)				
5US + 4DS	1.02 (US)	0.29 (DS)	0.90 (US)	0.18 (DS)	0.69 (US)	0.17 (DS)	0.31 (US)	0.16 (DS)	0.28 (US)			
5DS + 5US	0.27 (DS)	0.99 (US)	0.19 (DS)	0.88 (US)	0.19 (DS)	0.34 (US)	0.16 (DS)	0.31 (US)	0.12 (DS)	0.14 (US)		
6US + 5DS	1.0 (US)	0.28 (DS)	0.92 (US)	0.24 (DS)	0.71 (US)	0.16 (DS)	0.32 (US)	0.14 (DS)	0.28 (US)	0.14 (DS)	0.15 (US)	
6DS + 6US	0.30 (DS)	1.02 (US)	0.22 (DS)	0.91 (US)	0.18 (DS)	0.35 (US)	0.17 (DS)	0.29 (US)	0.13 (DS)	0.25 (US)	0.13 (DS)	0.19 (US)

Table 2
Transfer ratio (TR) values for different up and down strokes during the deposition of human serum albumin (HSA) multilayers.

Name of the films	TR values for the HSA layer deposition [US → up stroke and DS → down stroke]											
1US	1.05 (US)											
1DS + 1US	0.28 (DS)	0.97 (US)										
2US + 1DS	1.01 (US)	0.22 (DS)	0.86 (US)									
2DS + 2US	0.30 (DS)	0.97 (US)	0.21 (DS)	0.85 (US)								
3US + 2DS	0.96 (US)	0.25 (DS)	0.86 (US)	0.15 (DS)	0.70 (US)							
3DS + 3US	0.24 (DS)	0.91 (US)	0.18 (DS)	0.80 (US)	0.15 (DS)	0.26 (US)						
4US + 3DS	0.94 (US)	0.17 (DS)	0.80 (US)	0.14 (DS)	0.69 (US)	0.13 (DS)	0.24 (US)					
4DS + 4US	0.24 (DS)	0.93 (US)	0.17 (DS)	0.81 (US)	0.14 (DS)	0.30 (US)	0.12 (DS)	0.22 (US)				
5US + 4DS	0.95 (US)	0.19 (DS)	0.82 (US)	0.14 (DS)	0.65 (US)	0.14 (DS)	0.23 (US)	0.13 (DS)	0.23 (US)			
5DS + 5US	0.23 (DS)	0.94 (US)	0.16 (DS)	0.83 (US)	0.16 (DS)	0.29 (US)	0.12 (DS)	0.21 (US)	0.11 (DS)	0.13 (US)		
6US + 5DS	0.96 (US)	0.20 (DS)	0.81 (US)	0.15 (DS)	0.66 (US)	0.15 (DS)	0.24 (US)	0.14 (DS)	0.25 (US)	0.12 (DS)	0.13 (US)	
6DS + 6US	0.24 (DS)	0.95 (US)	0.17 (DS)	0.85 (US)	0.15 (DS)	0.27 (US)	0.13 (DS)	0.20 (US)	0.12 (DS)	0.13 (US)	0.11 (DS)	0.13 (US)

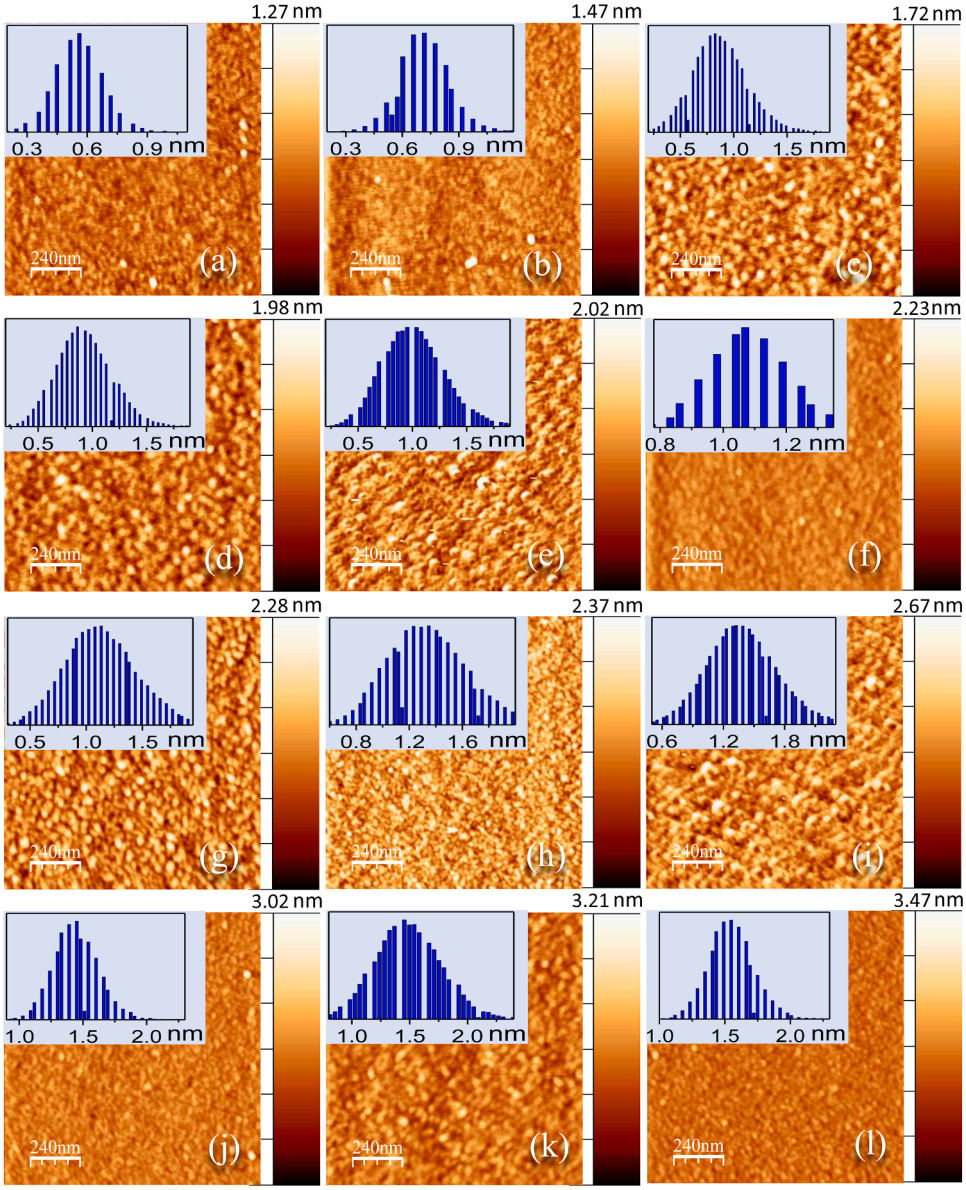

Fig. 2. AFM images obtained from the BSA films: (a) 1US, (b) 1DS+1US, (c) 2US+1DS, (d) 2DS+2US, (e) 3US+2DS, (f) 3DS+3US, (g) 4US+3DS, (h) 4DS+4US, (i) 5US+4DS, (j) 5DS+5US, (k) 6US+5DS and (l) 6DS+6US. Height or z-scale bars are shown on the right hand side of all images. Insets are the corresponding height histograms.

HSA multilayer depositions are shown as tabular form in Table 1 and Table 2 respectively.

AFM images depicting the surface topography of BSA and HSA monolayer to multilayer films deposited on Si (001) substrates are shown in Fig. 2 and Fig. 3 respectively. Surface topography of all BSA films, i.e., 1US to 6DS+6US BSA films are shown in Fig. 2. Similarly, all

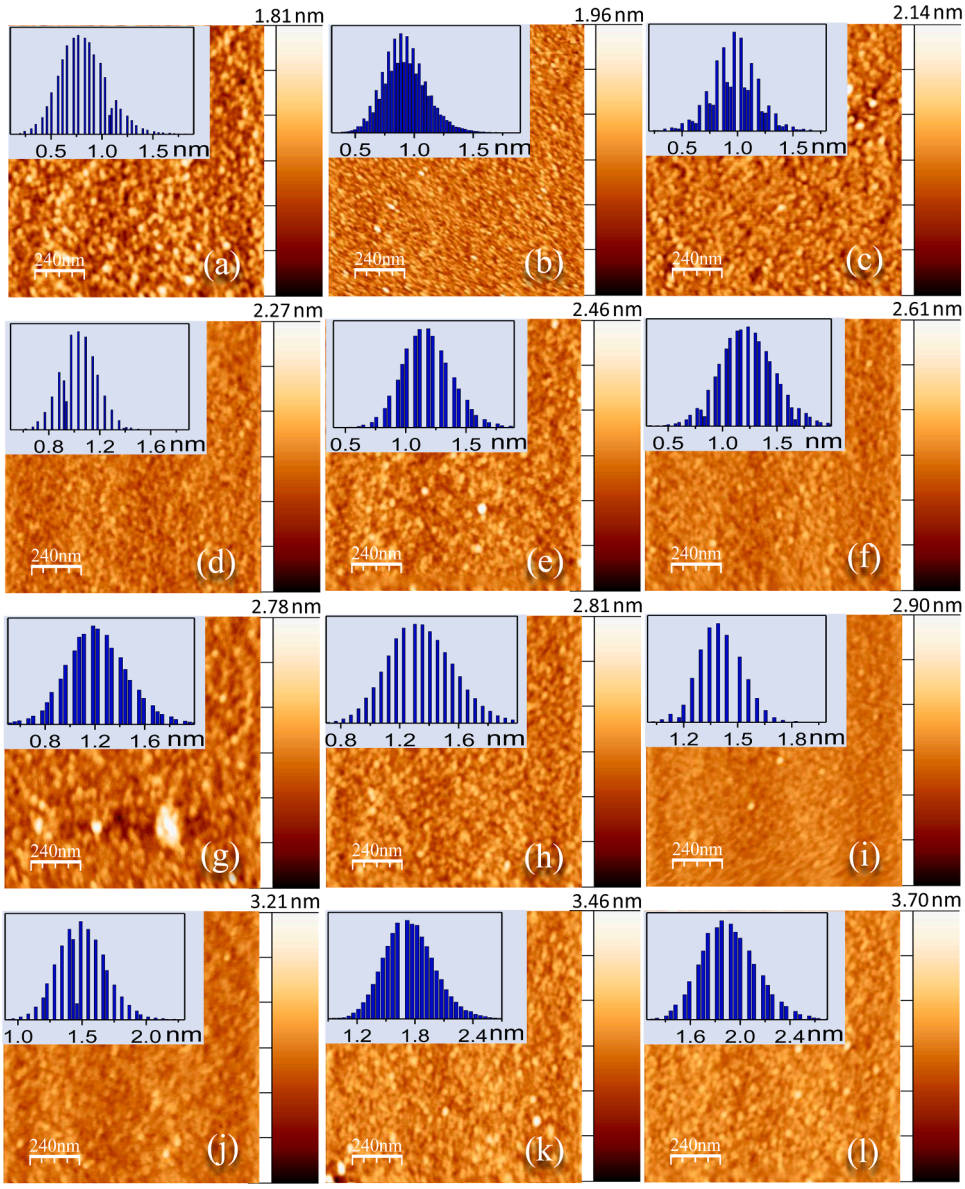

Fig. 3. AFM images obtained from the HSA films: (a) 1US, (b) 1DS+1US, (c) 2US+1DS, (d) 2DS+2US, (e) 3US+2DS, (f) 3DS+3US, (g) 4US+3DS, (h) 4DS+4US, (i) 5US+4DS, (j) 5DS+5US, (k) 6US+5DS and (l) 6DS+6US. Height or z-scale bars are shown on the right hand side of all images. Insets are the corresponding height histograms.

HSA films, i.e., 1US to 6DS+6US HSA films are shown in Fig. 3. For both the BSA and HSA films, AFM images were taken for a scan size of 1 × 1 μm^2. AFM images show nearly globular morphology for all the deposited films. To extract the height information from all the deposited films, total heights of all the films are shown by the height scale bars as shown on the right hand side of all the AFM images, whereas, the average height information are revealed by the height histograms which are shown in the insets of the corresponding figures. It can be seen from the height histograms that the average heights of BSA films deposited by the odd number of strokes, i.e., for 1US, 2US+1DS, 3US+2DS, 4US+3DS, 5US+4DS and 6US+5DS films are ≈ 0.57, 0.88, 1.04, 1.15, 1.40 and 1.51 nm, whereas, the corresponding total film heights are ≈ 1.27, 1.72, 2.02, 2.28, 2.67 and 3.21 nm respectively as obtained from the height scale bars. Similarly, for BSA films deposited by the even number of strokes, i.e., for 1DS+1US, 2DS+2US, 3DS+3US, 4DS+4US, 5DS+5US and 6DS+6US films, the average heights are obtained as ≈ 0.73, 0.94, 1.09, 1.36, 1.45 and 1.56 nm, whereas, the corresponding total film heights as obtained from the height scale bars are ≈ 1.47, 1.98, 2.23, 2.37, 3.02 and 3.47 nm respectively. Heights of all the HSA films are also extracted from both the height scale bars and height histograms. An average height of ≈ 0.83, 0.99, 1.19, 1.25, 1.40 and 1.77 nm are obtained from the HSA films deposited by the odd number of strokes, i.e., for 1US, 2US+1DS, 3US+2DS, 4US+3DS, 5US+4DS and 6US+5DS films, whereas, the corresponding total film heights as obtained from the height scale bars are ≈ 1.81, 2.14, 2.46, 2.78, 2.90 and 3.46 nm respectively. HSA films deposited by the even number of strokes, i.e., for 1DS+1US, 2DS+2US, 3DS+3US, 4DS+4US, 5DS+5US and 6DS+6US films, the average heights of ≈ 0.93, 1.04, 1.25, 1.35, 1.51 and 1.92 nm are obtained, whereas, the corresponding total heights are ≈ 1.96, 2.27, 2.61, 2.81, 3.21 and 3.70 nm respectively. AFM images of both the BSA and HSA films thus show that the film morphologies are nearly similar and their height information reveals that as the number of up and down stroke increases, the thickness of the deposited films also increases gradually but by a very small amount. It is also found from the AFM analysis that relatively higher thickness is obtained from the HSA films as probably the defects corresponding to more or less compact films, are

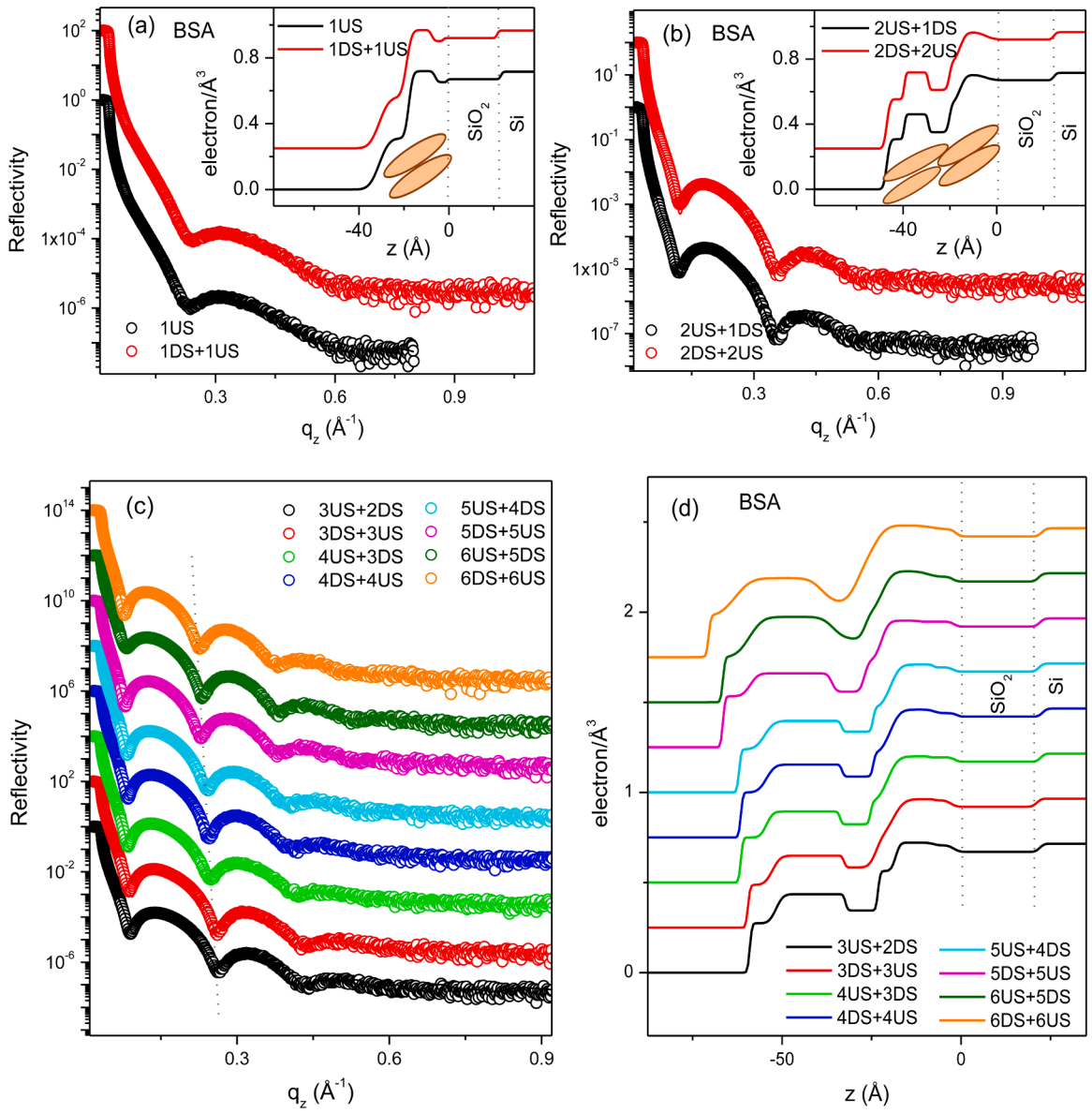

Fig. 4. X-ray reflectivity data (open circles) and corresponding fitted curves (solid lines) of (a) 1US and 1US+1DS, (b) 2US+1DS and 2DS+2US and (c) 3US+2DS to 6DS+6US BSA films. (d) Electron density profiles (EDPs) obtained from the 3US+2DS to 6DS+6US films. Insets: corresponding electron density profiles. Reflectivity data, fitted curves and EDPs are shifted vertically for clarity.

deposited for the HSA films, which also agrees well with the lower value of the electron density obtained from the XRR analysis that will be discussed in the subsequent sections.

Out-of-plane structures of the BSA and HSA films deposited using up stroke and different numbers of down-up and up-down cycles of the substrate by LB method are obtained from the X-ray reflectivity analysis. X-ray reflectivity data (open circles) and the corresponding fitted curves (solid lines) of BSA and HSA films for 1US, 1DS+1US, 2US+1DS and 2DS+2US films are shown in Fig. 4 and Fig. 5 respectively. The EDPs obtained from the XRR data for both the protein molecules are shown in the insets of the corresponding figures. It is clear from the reflectivity data and EDPs which are shown in Fig. 4(a) that the out-of-plane structure remains nearly unchanged for both the 1US and 1DS+1US films. EDP shows that only a single BSA molecular layer is deposited in the single up stroke, i.e., for 1US film. The monomolecular protein layer of thickness ≈ 37 Å (maximum electron density ≈ 0.72 electrons/Å^3) is shown as a cartoon inside the inset of Fig. 4(a). Thus, during the down stroke, BSA layer is not deposited on the hydrophilic Si (001) substrate as EDP of 1DS+1US film is nearly the same as 1US. Reflectivity profiles and EDPs of 2US+1DS and 2DS+2US films are also nearly similar as shown in Fig. 4(b) and it implies the formation of BSA bimolecular layer of thickness ≈ 49 Å (maximum electron densities are ≈ 0.70 and 0.45 electrons/Å^3 for lower and upper layer), which is again shown as a cartoon in the inset of Fig. 4(b). It thus again implies that the deposition in the down stroke is not taking place. Like BSA, for HSA also the deposition is not taking place in the down stroke and as a result the out-of-plane structures of the 1US and 1DS+1US films are similar and such structural similarity also exist for 2US+1DS and 2DS+2US films as shown in Fig. 5(a) and 5(b). The X-ray reflectivity profiles of all the remaining BSA films, i.e., of 3US+2DS, 3DS+3US, 4US+3DS, 4DS+4US, 5US+4DS, 5DS+5US, 6US+5DS and 6DS+6US are shown in Fig. 4(c) and the corresponding EDPs are shown in Fig. 4(d). From the EDPs it is again clear that the thicknesses of films 3US+2DS and 3DS+3US are nearly the same and after that from 4US+3DS to 6DS+6US films thickness increases by a very small amount gradually. This is also visible from the positions of the second dip in the reflectivity profiles as marked

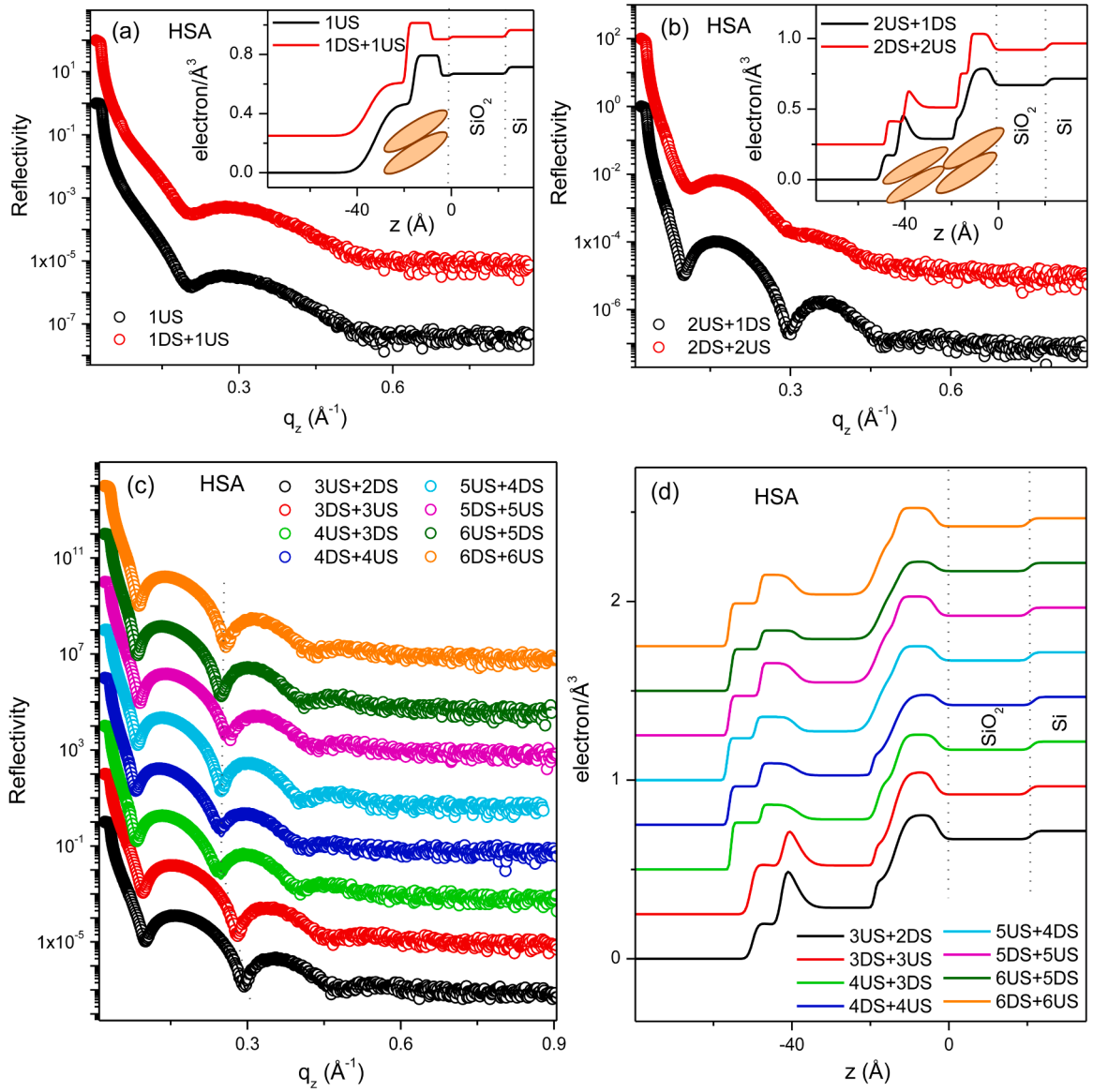

Fig. 5. X-ray reflectivity data (open circles) and corresponding fitted curves (solid lines) of (a) 1US and 1US+1DS, (b) 2US+1DS and 2DS+2US and (c) 3US+2DS to 6DS+6US HSA films. (d) Electron density profiles (EDPs) obtained from the 3US+2DS to 6DS+6US films. Insets: corresponding electron density profiles. Reflectivity data, fitted curves and EDPs are shifted vertically for clarity.

by the solid and dotted lines. From the EDPs it is also clear that the bimolecular layer structure formed for 2US+1DS or 2DS+2US films is maintained up to the 6DS+6US film, however, the thickness of the bimolecular layer slightly increases possibly due to an increase of individual molecular tilting taking place during up/down strokes. The thickness increment is higher for 3US+2DS and 3DS+3US films (≈ 10 Å) and after that the thickness increment relatively decreases for each consecutive up and down strokes, however, finally for the 6DS+6US film the thickness becomes ≈ 71 Å, i.e., the amount of possible thickness increment is ≈ 34 Å, although the bimolecular structure is maintained in the deposited film. The maximum electron densities in the lower and upper layers of the 6DS+6US film become ≈ 0.73 and 0.44 electrons/Å^3 respectively. Like BSA, for HSA also all reflectivity profiles from 3US+2DS to 6DS+6US are shown in Fig. 5(c) and the corresponding EDPs are shown in Fig. 5(d). The positions of the second dip in the reflectivity profiles are also marked by the solid and dotted lines. From EDPs it is clear that the thickness of the films 3US+2DS and 3DS+3US are nearly the same and for these films the thickness is increased by ≈ 2-3 Å and after that the film thickness is increased by such a small amount that for the 6DS+6US film the thickness finally becomes ≈ 57 Å, i.e., the increment in the thickness amount is ≈ 7-8 Å. The maximum electron densities in the lower and upper layers of the 6DS+6US film become ≈ 0.77 and 0.40 electrons/Å^3 respectively. Variation of the film thicknesses and values of integrated electron densities, i.e., electrons/Å^2 obtained from the EDPs with an increasing number of up and down strokes for both the BSA and HSA films are shown in Fig. 6(a) and 6(b) respectively. The structure of the protein film before the plateau is also obtained by depositing the protein layer on hydrophilic Si (001) surface in single up stroke at 5 mN/m. From the EDPs obtained from the data fitting it is clear that only monolayer is deposited, but the molecular tilting is relatively less as relatively lower thickness is obtained than the film deposited at higher surface pressure (17 mN/m) in single up stroke (data not shown). Here it is important to mention that during protein adsorption on solid surface from protein solutions, it is found that after adsorption, the protein molecules changes their structure from globular to disc as lateral spreading takes place due to rearrangement of secondary or ternary structures [45,46]. However, it is also concluded in the work that with time such spreading occurs depending upon the

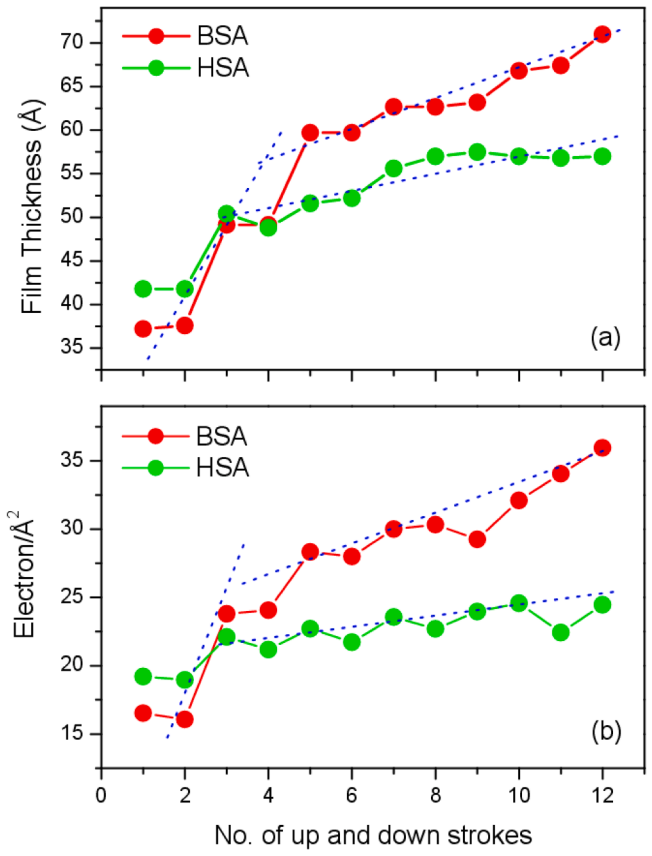

Fig. 6. Variation of the film thickness and integrated electron density (electrons/Å2) obtained from BSA and HSA films with increasing number of up and down strokes.

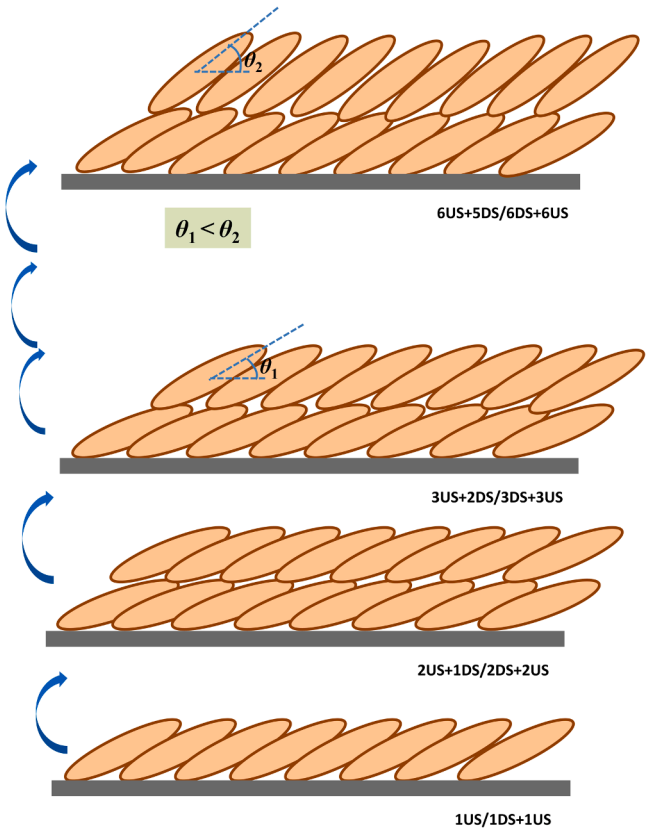

Fig. 7. Schematic representation of the protein (BSA, HSA) layer growth on solid substrate with increasing number of up and down strokes under LB method. After bimolecular layer formation the layer thickness increases as the molecular tilting increases with respect to the substrate surface.

availability of space but significant amount of structure still remains unaltered [45,46]. Such structural rearrangement as found in standard protein adsorption process from protein solution may not take place in LB deposition as in the LB method protein layer is deposited on a solid surface from a relatively compact protein monolayer and as a result such structural modification is hindered. Therefore, molecular tilting is the most probable reason for such thickness and electron density variation of the protein layers.

The thickness and electrons/Å^2 variations for BSA and HSA are slightly different as obtained from the Fig. 6. For BSA, the thickness of the films increases by higher amounts initially and then there is a slight increment with up/down strokes, which are marked by blue dotted lines. The density growth also matches with the same trend of film thickness increment. Such film growth with increase in the number of up/down strokes can be explained in the molecular level from EDPs. Only one molecular layer of BSA is deposited at 17 mN/m in the single up stroke and considering the oblate ellipsoid structure of BSA it can be considered that one tilted molecular layer is formed. In the down stroke, no molecular layer is deposited as EDPs of both the 1DS+1US and 1US films are same. In the 2US+1DS, i.e., for up-down-up cycle, one more molecular layer is deposited on top of the lower molecular layer as observed from the EDP and the molecules are tilted in both the layers. Again as the deposition is not possible in the down stroke, so EDPs are nearly same for both the 2US+1DS and 2DS+2US films. Although for 3US+2DS film, i.e., for up-down-up-down-up cycle the thickness is increased but EDP confirms that any more layer is not formed on top of the bimolecular layer formed before. The increased value of film thickness and integrated electron density value implies that as molecules are more tilted (with respect to substrate surface) so more numbers of molecules are deposited in the gaps as formed due to molecular tilting.

After that, with an increase in the number of up/down strokes only the amount of tilting increases gradually but by a very small amount and accordingly the new molecules are deposited in the vacant positions originating due to this molecular tilting. Variation of molecular tilting possibly occurs due to the effect of water surface tension during the passing of the film covered substrate through the air-water interface. It has also been found by other groups that the liquid surface tension can drive the crystallographic orientation of initially randomly oriented particles [47]. The growth of BSA layers with an increasing number of up/down strokes is illustrated in a cartoon presented in Fig. 7. For HSA molecules, the growth is similar to BSA, but the thickness increment is relatively lower for HSA layers after bimolecular layer formation with increasing up/down strokes. Probability of molecular tilting is quite lower or negligible and accordingly significantly lower numbers of HSA molecules are deposited in the bimolecular layer. Such small difference between BSA and HSA growth nature is related to their hydrophilic/hydrophobic nature at the molecular level as it is known that HSA molecular surface is more hydrophobic in nature than BSA molecular surface [48]. Thus, considering thickness and electron density, the growth mode of BSA and HSA monolayer on hydrophilic silicon surface under conventional Langmuir-Blodgett deposition can be predicted. It is clear that only two molecular layers are deposited due to up-down-up or down-up-down-up cycles but after that only amount of molecular tilting increases and as a result layer thickness increases and more number of molecules are deposited in the vacant position but no extra molecular layer or islands are developed above the bimolecular layer. These features of growth of BSA/HSA Langmuir monolayer under Langmuir-Blodgett deposition have a strong similarity with the interrupted layer-by-layer or FM growth mode where an interruption in deposition occurs after bimolecular layer formation. AFM images have

also not provided any island-like patches or structures after bimolecular layer as nearly the smooth globular-like morphology is obtained from the multiple up/down strokes. Thus, although layer-by-layer or FM growth mode is common for the LB growth but for the BSA and HSA protein layer deposition it is interrupted after bimolecular layer formation and due to that further molecular layer deposition was not possible. However, in this method most compact bimolecular protein layer formation is possible. Probably the hydrophilic substrate and hydrated protein interaction ($F_{S\text{-}HP}$) is stronger than the water and hydrated protein interaction ($F_{W\text{-}HP}$) and as a result monomolecular layer deposition was possible in single up stroke. On the other hand, the interaction between the dehydrated protein deposited on the solid substrate and hydrated protein on the water surface ($F_{DP\text{-}HP}$) is relatively weaker than the $F_{W\text{-}HP}$ and as a result deposition was not possible during the down stroke. It is unclear why molecular layers are not deposited in fifth and subsequent up stokes after bimolecular layer formation although it is similar like third up stroke. It may be related with the coverage of the upper layer of the protein bimolecular layer. As the coverage of the upper layer is around 60-64% in comparison with the lower layer (considering 100% coverage for the lower layer density), so there is a vacancy of 36-40% in the upper layer and most probably such vacancy is symmetrical around each deposited molecule. Such amount of molecular vacancy may have reduced the interaction ($F_{HP\text{-}HP}$) between the hydrated protein molecules, i.e., $F_{HP\text{-}HP}$ becomes less than $F_{W\text{-}HP}$ and as a result deposition of the molecular layer is not possible above the bimolecular layer after third up stroke. It is likely that the molecular layer formation of these globular proteins is related with the threshold value (more than 66%) of the two-dimensional percolated structure [49-51] and as the coverage of the upper layer is less than around 66%, so symmetrical vacant positions are formed that reduces the $F_{HP\text{-}HP}$ and as a result interrupted FM growth mode is evidenced. Thus, under this conventional LB method highly compact bimolecular protein layer deposition is possible which may have potential applications.

4. Conclusions

π–A isotherms of globular proteins BSA and HSA are studied at aqueous subphase pH of ≈ 7.0, well above the isoelectric point (≈ 4.8) of both the protein molecules. The nature of both the isotherms is almost similar except the path of reaching maximum pressure values. Stability curves (A/A_0-t) show that for the same constant pressure, the area loss by HSA monolayer is less than that of BSA monolayer, however, the deposition of layers over a long period of time is possible from both the protein monolayers. Compact protein films are deposited by successive up and down strokes of the substrate through the monolayer covered aqueous subphase continuing up to twelve numbers of up and down strokes, i.e., from 1US to 6DS+6US films. AFM images of BSA and HSA films show nearly globular morphology and their corresponding heights reveals that the thickness of the deposited films increases slightly with increase in the number of up and down strokes. X-ray reflectivity analysis shows that thickness of 1US and 1US+1DS, 2US+1DS and 2DS+2US, 3US+2DS and 3DS+3US are almost same, i.e., deposition is not possible during down stroke, while from 4US+3DS to 6DS+6US films the thickness gradually increases but by a very small amount. EDPs obtained from the X-ray reflectivity data shows that there is a slight variation in increment of thickness and electrons per unit area of the BSA films than that of HSA. The increment in thickness and electrons per unit area is due to the tilting of the protein molecules and occupying the vacant spaces produced by such molecular tilting in successive up and down strokes. However, highly compact bimolecular protein layer deposition is possible in this method, which may have potential applications. Considering the thickness and density variation of BSA and HSA films obtained from both EDPs and AFM study it is clear that interrupted layer-by-layer or FM growth mode is followed in such protein deposition under the conventional LB method.

Author's contribution

RJS, BKS and SK wrote the manuscript. RJS performed the experiments and all jointly analysed the data. SK supervised the work and all approved the manuscript.

Declaration of Competing Interest

The authors declare that they have no known competing financial interests or personal relationships that could have appeared to influence the work reported in this paper.

Acknowledgements

Authors acknowledge the financial support from Department of Science and Technology, Govt. of India.

References

[1] J. Kim, R. Yamasaki, J. Park, H. Jung, H. Lee, T. Kawai, Highly Dense Protein Layers Confirmed by Atomic Force Microscopy and Quartz Crystal Microbalance, J, Biosci. Bioeng. 97 (2004) 138–140, https://doi.org/10.1016/S1389-1723(04)70182-6.
[2] J. Voros, The Density and Refractive Index of Adsorbing Protein Layers, Biophys. J 87 (2004) 553–561, https://doi.org/10.1529/biophysj.103.030072.
[3] A.P. Girard-Egrot, S. Godoy, L.J Blum, Enzyme association with lipidic Langmuir-Blodgett films: Interests and applications in Nanobioscience, Adv. Colloid Interface Sci 116 (2005) 205–225, https://doi.org/10.1016/j.cis.2005.04.006.
[4] F. Beigi, P. Lundahl, Immobilized biomembrane chromatography of highly lipophilic Drugs, J, Chromatogr. A 852 (1999) 313–317, https://doi.org/10.1016/S0021- 9673(99)00025-4.
[5] Y. Okahata, T. Tsuruta, K. Ijiro, K. Ariga, Langmuir-Blodgett Films of an Enzyme-Lipid Complex for Sensor Membranes, Langmuir 4 (1988) 1373–1375, https://doi.org/10.1021/la00084a030.
[6] J.J. Ramsden, Biomimetic protein immobilization using lipid bilayers, Biosensors & Bioelectronics 13 (1998) 593–598, https://doi.org/10.1016/S0956-5663(98)00014-1.
[7] S. Hou, J. Wang, C.R. Martin, Template-Synthesized Protein Nanotubes, Nano Lett 5 (2004) 231–234, https://doi.org/10.1021/nl048305p.
[8] Z. Siwy, L. Trofin, P. Kohli, L.A. Baker, C. Trautmann, C.R. Martin, Protein Biosensors Based on Biofunctionalized Conical Gold Nanotubes, J. Am. Chem. Soc. 127 (2005) 5000–5001, https://doi.org/10.1021/ja043910f.
[9] C. Leger, P. Bertrand, Direct Electrochemistry of Redox Enzymes as a Tool for Mechanistic Studies, Chem. Rev 108 (2008) 2379–2438, https://doi.org/10.1021/cr0680742.
[10] G.D. Fasman, in: G.D. Fasman (Ed.), Plenum Press, New York, 1989, pp. 193–316.
[11] M.J. Sippl, Calculation of Conformational Ensembles from Potentials of Mean force, J. Mol. Biol. 213 (1990) 859–883, https://doi.org/10.1016/S0022-2836(05)80269-4.
[12] F. Moreno, M. Cortljo, J. Gonzalez-Jimenez, Interaction of Acrylodan with Human Serum Albumin. A Fluorescence Spectroscopic Study, Photochemistry and Photobiology 70 (1999) 695–700, https://doi.org/10.1111/j.1751-1097.1999.tb08272.x.
[13] D.C. Carter, J.X. Ho, Structure of Serum Albumin, Advances in Protein Chemistry 45 (1994) 153–203, https://doi.org/10.1016/S0065-3233(08)60640-3.
[14] F. Macritchie, L. Ter-Minassian-Saraga, Concentrated protein monolayers: desorption studies with radiolabelled bovine serum albumin, Colloids and Surfaces 10 (1984) 53–64, https://doi.org/10.1016/0166-6622(84)80007-4.
[15] C.A. Haynes, W. Norde, Globular proteins at solid/liquid interfaces, Colloids and Surfaces B: Biointerfaces 2 (1994) 517–566, https://doi.org/10.1016/0927- 7765(94)80066-9.
[16] T. Kamilya, P. Pal, G.B. Talapatra, Interaction of Ovalbumin with Phospholipids Langmuir-Blodgett Film, J. Phys. Chem. B 111 (2007) 1199–1205, https://doi.org/10.1021/jp063377l.
[17] T. Kamilya, P. Pal, M. Mahato, G.B. Talapatra, Fabrication of Ovalbumin–Phospolipid Thin Film with Minimal Protein Aggregation by Different Self-Assembly Methods, J, Nanosci. Nanotechnol. 9 (2009) 2956–2964, https://doi.org/10.1166/jnn.2009.dk23.
[18] T. Kamilya, P. Pal, M. Mahato, G. B. Talapatra, Immobilization and the conformational study of phospholipid and phospholipid-protein vesicles Materials Science and Engineering C 29 (2009) 1480–1485.10.1016/j.msec.2008.12.003.
[19] K. Ariga, J.P. Hill, M.V. Lee, A. Vinu, R. Charvet, S. Acharya, Challenges and breakthroughs in recent research on self-assembly, Sci. Technol. Adv. Mater 9 (2008), 014109, https://doi.org/10.1088/1468-6996/9/1/014109.
[20] P. Pal, D. Nandi, T.N. Misra, Immobilization of alcohol dehydrogenase enzyme in a Langmuir-Blodgett film of stearic acid: its application as an ethanol sensor, Thin Solid Films 239 (1994) 138–143, https://doi.org/10.1016/0040-6090(94)90120-1.

[21] F. MacRitchie, L. Ter-Minassian-Saraga, Stability of highly compressed spread monolayers of ^{125}I-labelled and cold BSA, Progr. Colloid & Polymer Sci 68 (1983) 14–19, https://doi.org/10.1007/BFb0114134.
[22] L.R.S. Barbosa, M.G. Ortore, F. Spinozzi, P. Mariani, S. Bernstorff, R. Itri, The Importance of Protein-Protein Interactions on the pH-Induced Conformational Changes of Bovine Serum Albumin: A Small-Angle X-Ray Scattering Study, Biophysical Journal 98 (2010) 147–157, https://doi.org/10.1016/j.bpj.2009.09.056.
[23] J.H. Clark, Reversible crystallization in tendons and its Functional significance, Physiology 14 (1928) 526–532, https://doi.org/10.1073/pnas.14.7.526.
[24] R. Androsch, B. Wunderlich, Reversible Crystallization and Melting at the Lateral Surface of Isotactic Polypropylene Crystals, Macromolecules 34 (2001) 5950–5960, https://doi.org/10.1021/ma010260g.
[25] T.J. Su, J.R. Lu, R.K. Thomas, Z.F. Cui, J. Penfold, The Conformational Structure of Bovine Serum Albumin Layers Adsorbed at the Silica-Water Interface, J. Phys. Chem. B 102 (1998) 8100–8108, https://doi.org/10.1021/jp981239t.
[26] X. Wang, Y. Zhang, J. Wu, M. Wang, G. Cui, J. Li, G. Brezesinski, Dynamical and morphological studies on the adsorption and penetration of human serum albumin into phospholipid monolayers at the air/water interface, Colloids and Surfaces B: Biointerfaces 23 (2002) 339–347, https://doi.org/10.1016/S0927-7765(01)00269-7.
[27] I. Daruka, A.L. Barabasi, Dislocation-Free Island Formation in Heteroepitaxial Growth: A Study at Equilibrium, Physical Review Letters 79 (1997) 3708–3711, https://doi.org/10.1103/PhysRevLett.79.3708.
[28] V.A. Shchukin, D. Bimberg, Spontaneous ordering of nanostructures on crystal surfaces, Rev. Mod. Phys 71 (1999) 1125–1171, https://doi.org/10.1103/RevModPhys.71.1125.
[29] C. Lorch, J. Novak, R. Banerjee, S. Weimer, J. Dieterle, C. Frank, A. Hinderhofer, A. Gerlach, F. Carla, F. Schreiber, Influence of C_{60} co-deposition on the growth kinetics of diindenoperylene–From rapid roughening to layer-by-layer growth in blended organic films, J. Chem. Phys. 146 (2017), 052807, https://doi.org/10.1063/1.4966583.
[30] D.G. de Oteyza, E. Barrena, Y. Zhang, T.N. Krauss, A. Turak, A. Vorobiev, H. Dosch, Experimental Relation between Stranski-Krastanov Growth of DIP/F_{16}CoPc Heterostructures and the Reconstruction of the Organic Interface, J. Phys. Chem. C 113 (2009) 4234–4239, https://doi.org/10.1021/jp809512a.
[31] X. Zhang, E. Barrena, D. Goswami, D.G. de Oteyza, C. Weis, H. Dosch, Evidence for a Layer-Dependent Ehrlich-Schwobel Barrier in Organic Thin Film Growth, Physical Review Letters 103 (2009), 136101, https://doi.org/10.1103/PhysRevLett.103.136101.
[32] J.K. Basu, S. Hazra, M.K. Sanyal, Growth Mechanism of Langmuir- Blodgett Films, Phys. Rev. Lett 82 (1999) 4675–4678, https://doi.org/10.1103/PhysRevLett.82.4675.
[33] X.-H. Li, M. Li, Z.-H Mai, Kinetic roughening of the interfaces of Langmuir-Blodgett Films, Phys. Rev. B 69 (2004), 235407, https://doi.org/10.1103/PhysRevB.69.235407.
[34] S. Kundu, A. Datta, S. Hazra, Growth of a collapsing Langmuir monolayer, Phys. Rev. E 73 (2006), 051608, 10.1103.73.051608.
[35] R.K. Gupta, K.A. Suresh, AFM studies on Langmuir-Blodgett films of cholesterol, Eur. Phys. J. E 14 (2004) 35–42, https://doi.org/10.1140/epje/i2003-10088-4.
[36] L.A. Sklar, B.S. Hudson, R.D. Simoni, Conjugated Polyene Fatty Acids as Fluorescent Probes: Binding to Bovine Serum Albumin, Biochemistry 16 (1977) 5100–5108, https://doi.org/10.1021/bi00642a024.
[37] I. Horcas, R. Fernández, J.M. Gómez-Rodríguez, J. Colchero, J. Gómez-Herrero, A. M. Baró, WSXM: A software for scanning probe microscopy and a tool for nanotechnology, Review of Scientific Instruments 78 (2007), 013705, https://doi.org/10.1063/1.2432410.
[38] L.G. Parratt, Surface Studies of Solids by Total Reflection of X-Rays, Physical Review 95 (1954) 359–369, https://doi.org/10.1103/PhysRev.95.359.
[39] A. Gibaud, Specular Reflectivity from Smooth and Rough Surfaces, In: X-ray and Neutron Reflectivity: Principles and Applications, J. Daillant, A. Gibaud, ed., Springer-Verlag (1999) 87–120, https://doi.org/10.1007/3-540-48696-8_3.
[40] M. Tolan, Reflectivity of X-Rays from Surfaces. In Reflectivity of X-rays from Surfaces, Springer, Berlin, 1999, https://doi.org/10.1007/BFb0112836.
[41] J.K. Basu, M.K. Sanyal, Ordering and growth of Langmuir–Blodgett films: X- ray Scattering studies, Physics Reports 363 (2002) 1–84, https://doi.org/10.1016/S0370- 1573(01)00083-7.
[42] S. Kundu, A. Datta, M.K. Sanyal, J. Daillant, D. Luzet, C. Blot, B. Struth, Growth of bimolecular films of three-tailed amphiphiles, Physical Review E 73 (2006), https://doi.org/10.1103/PhysRevE.73.061602, 061602-1 – 061602-6.
[43] S. Kundu, A. Datta, S. Hazra, Effect of Metal Ions on Monolayer Collapses, Langmuir 21 (2005) 5894–5900, https://doi.org/10.1021/la0505770.
[44] S. Kundu, K. Das, V.K. Aswal, Modification of attractive and repulsive interactions among proteins in solution due to the presence of mono-, di- and tri-valent ions, Chem. Phys. Lett 578 (2013) 115–119, https://doi.org/10.1016/j.cplett.2013.05.062.
[45] W. Norde, C.E. Giacomelli, Conformational changes in proteins at interfaces: from solution to the interface, and back, Macromol. Symp 145 (1999) 125–136, https://doi.org/10.1002/masy.19991450114.
[46] W. Norde, Adsorption of Proteins at Solid-Liquid Interfaces, Cells and Materials 5 (1995) 97–112.
[47] N.R. Chevalier, P. Guenoun, Surface Tension Drives the Orientation of Crystals at the Air−Water Interface, J. Phys. Chem. Lett. 7 (2016) 2809–2813, https://doi.org/10.1021/acs.jpclett.6b01312.
[48] L. Ianeselli, F. Zhang, M.W.A. Skoda, R.M.J. Jacobs, R.A. Martin, S. Callow, S. Prevost, F. Schreiber, Protein-Protein Interactions in Ovalbumin Solutions Studied by Small-Angle Scattering: Effect of Ionic Strength and the Chemical Nature of Cations, J. Phys. Chem. B 114 (2010) 3776–3783, https://doi.org/10.1021/jp9112156.
[49] G.R. Grimmett, In Percolation. Springer-Verlag, New York, 1999.
[50] D. Stauffer, A. Aharony, In Introduction to Percolation Theory, Taylor & Francis, Washington, DC, 1992.
[51] D.J. Jacobs, M.F. Thorpe, Generic rigidity percolation in two dimensions, Phys. Rev. E 53 (1996) 3682, 10.1103.53.3682.